

## Using pollen in turbidites for vegetation reconstructions

LAURA S. MCDONALD,<sup>1\*</sup> LORNA J. STRACHAN,<sup>1</sup> KATHERINE HOLT,<sup>2</sup> ADAM D. MCARTHUR,<sup>3</sup> PHILIP M. BARNES,<sup>4</sup> KATHERINE L. MAIER,<sup>4</sup> ALAN R. ORPIN,<sup>4</sup> MARK HORROCKS,<sup>1,5</sup> ARATRIKA GANGULY,<sup>1</sup> JENNI L. HOPKINS<sup>6</sup> and HELEN C. BOSTOCK<sup>7</sup>

<sup>1</sup>School of Environment, University of Auckland-Waipapa Taumata Rau, Auckland-Tāmaki Makaurau, Aotearoa, New Zealand

<sup>2</sup>School of Agriculture and Environment, Massey University-Te Kunenga ki Pūrehuroa, Palmerston North-Te Papaioea, Aotearoa, New Zealand

<sup>3</sup>School of Earth and Environment, University of Leeds, Leeds, UK

<sup>4</sup>National Institute of Water and Atmospheric Research-Taihoru Nukurangi, Wellington-Te Whanganui a Tara, Aotearoa, New Zealand

<sup>5</sup>Microfossil Research Ltd, Auckland-Tāmaki Makaurau, Aotearoa, New Zealand

<sup>6</sup>School of Geography, Environment and Earth Sciences, Victoria University of Wellington - Te Herenga Waka, Wellington-Te Whanganui a Tara, Aotearoa, New Zealand

<sup>7</sup>School of the Environment, University of Queensland, Brisbane, Queensland, Australia

Received 23 April 2024; Revised 16 July 2024; Accepted 14 August 2024

**ABSTRACT:** Turbidites, deposited by sub-aqueous gravity flows, are common in sedimentary archives worldwide and present a unique challenge and opportunity when reconstructing past vegetation through pollen analysis. When sampling pollen from a sediment core for palaeovegetation records, it is common practice to target background sediments (i.e. pelagic sediment) and avoid sampling turbidites, as they are presumed to portray a misleading picture of past vegetation. This assumption stems from our limited understanding of pollen abundance and distribution through turbidites, meaning that palynologists overlook deposits that could potentially be used to reconstruct past vegetation and climate. We present pollen assemblage and sedimentological data from four recent (<150 years) deep marine turbidite deposits from the Hikurangi Subduction Margin, Aotearoa-New Zealand, with the aim of understanding the abundance and distribution of pollen in fine-grained turbidites. We find that pollen is diluted in the bases of turbidites, but despite this dilution, the proportions of different pollen taxa remain consistent through each turbidite. These results confirm that pollen can be sampled from turbidites for palaeovegetation reconstructions and that sampling the fine-grained upper parts of turbidites will provide the best pollen recovery.

© 2024 The Author(s) *Journal of Quaternary Science* Published by John Wiley & Sons Ltd.

**KEYWORDS:** Hikurangi Subduction Margin; pollen sampling; sediment sorting; turbidites; vegetation reconstruction

### Introduction

Submarine gravity flows, including turbidity currents, are responsible for transporting volumetrically more sediment globally than any other sedimentary transport process (Talling et al., 2007, 2012). Consequently, turbidites, the deposits of turbidity currents, are common in sedimentary archives worldwide (Beaudouin et al., 2004; Pouderoux et al., 2012a, 2012b; Webster et al., 2012; Gutiérrez-Pastor et al., 2013; Strachan et al., 2016; Vieira and Jolley, 2020; Jolley et al., 2022; Woodhouse et al., 2022). Despite the occurrence of turbidites in many sedimentary records, little is understood about the abundance or distribution of pollen within these deposits. It is common practice for palynologists to target background sediments (i.e. pelagic sediment) and avoid sampling turbidites when creating palaeovegetation records. This is because turbidites are often thought to provide a distorted representation of past vegetation, primarily due to the perception that the deposits favour hydrodynamically efficient pollen types (McGann, 2018) and possibly contain reworked pollen from

older deposits. On many tectonically active margins like the Hikurangi Subduction Margin, Aotearoa-New Zealand, sediment transport is dominated by turbidity currents, resulting in sediment cores with regular turbidites (Fig. 1; Pouderoux et al., 2012a, 2012b; Mountjoy et al., 2018; Howarth et al., 2021; Hayward et al., 2022a; Woodhouse et al., 2022; Maier et al., 2024). By excluding turbidites from pollen sampling strategies in sediment cores like these, volumetrically significant portions of the core would remain unsampled and, therefore, not represented in the final vegetation record. Furthermore, turbidites have been found to be rich in pollen and other organic matter (Vieira and Jolley, 1993, 2020; McArthur et al., 2017; Porro, 2018; Beaudouin et al., 2004; Jolley et al., 2022). Therefore, by omitting turbidites from climate proxy sampling strategies, we are overlooking deposits that could potentially help with reconstructions of past vegetation and climate. In order to sample pollen in turbidites for vegetation reconstructions, we need to better quantify pollen abundance in turbidites and understand how different pollen taxa are distributed through turbidites. For example, if pollen taxa are sorted in turbidites, a singular pollen sample from a deposit could bias the interpretation of past vegetation from a sedimentary record. To determine whether accurate pollen-based vegetation records can be obtained by sampling turbidites, we use a combination of

Correspondence: Laura S. McDonald, as above.

Email: laura.mcdonald@auckland.ac.nz

Current address: Katherine L. Maier, Pacific Northwest National Laboratory, Richland, WA 99354, USA.

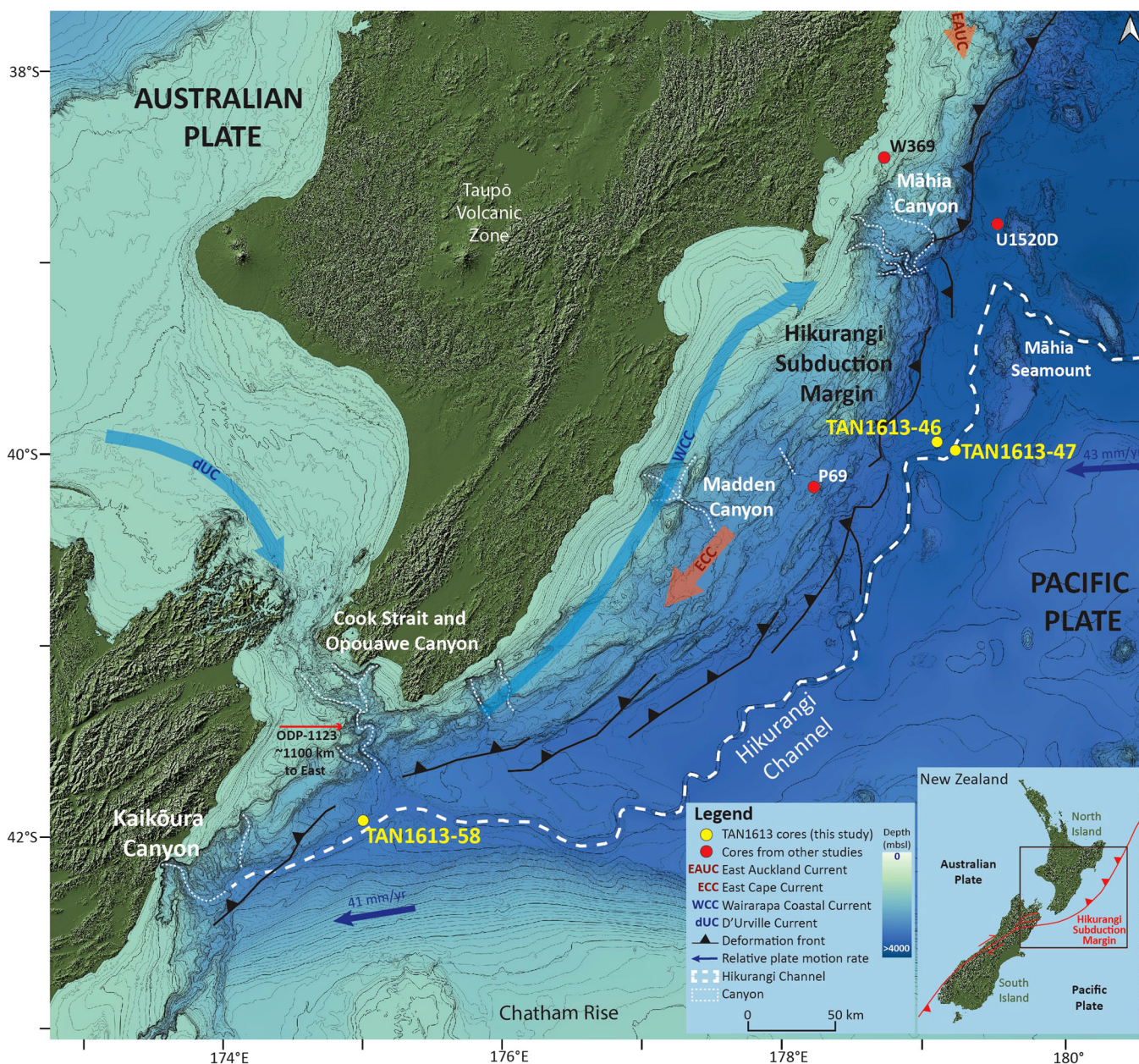


**Figure 1.** The Hikurangi Subduction Margin with the locations of the three TAN1613 sediment cores used in this study. Also mapped are other cores referred to in this study, including W369 (Wilmshurst et al., 1999), P69 (McGlone, 2001) (ODP-1123 (Mildenhall, 2003) is outside of the map area). [Color figure can be viewed at [wileyonlinelibrary.com](https://onlinelibrary.wiley.com)]

sedimentary core analyses and pollen assemblage analysis to determine which pollen<sup>1</sup> taxa are present and in what quantities in recent (<150 years) turbidites on the Hikurangi Subduction Margin (Fig. 1). Additionally, we use pollen distribution within the turbidites to interpret the flow dynamics of the depositing turbidity currents, and we propose guidelines for sampling pollen in turbidites to create palaeovegetation records.

In the context of turbidity currents, pollen behaves hydrodynamically as a silt-sized particle, meaning it can be considered as a grain during sediment transport processes (Muller, 1959; Tyson, 1995; Beaudouin et al., 2004). Porro (2018) found that in sand-silt turbidites, pollen is concentrated in the silt-rich upper part of turbidites. Many modern turbidite systems are confined to the slope (Harris and Whiteway, 2011) depositing fine-grained turbidites (silt-clay), raising the question of whether pollen is also

sorted in fine-grained turbidites as in coarser-grained (sand-rich) turbidites (Porro, 2018). Prior to this study, no other published studies have sampled pollen at a high resolution to understand how it varies through fine-grained turbidites. Due to the variable densities, sizes and complex morphologies of pollen grains (Holmes, 1990; Mildenhall, 2003), it is reasonable to expect that pollen taxa may experience differential sorting in turbidites. For example, air and water settling experiments (Di-Giovanni et al., 1995; Hirose and Osada, 2016) have found that saccate<sup>2</sup> pollen (e.g. *Pinus* and many Podocarpaceae) take longer to settle than other non-saccate pollen and can therefore float for long distances (Heusser and Balsam, 1977; Holmes, 1990; Tomlinson, 1994; Mildenhall, 2003; Montade et al., 2011; McGann, 2018). Additionally, due to their robustness, fern spores (e.g. *Cyathea*) tend to be over-represented in marine sedimentary records offshore Aotearoa-New Zealand (Wilmshurst et al., 1999;

<sup>1</sup>In this study, we use the term pollen to collectively refer to both pollen and spores from terrestrial plants (i.e. Angiosperms, Gymnosperms, Pteridophytes, etc.).

<sup>2</sup>Saccate pollen have sacs that are commonly filled with air making them buoyant and 'non-wettable'.

McGlone, 2001; Carter et al., 2002; Elliot et al., 2003; Mildenhall, 2003; Orpin et al., 2006; Crouch et al., 2010). Fern spores are also suggested to be denser than Podocarpaceae pollen due to being non-saccate and typically relatively large (~45 µm; McArthur et al., 2016). As grains begin to settle from a decelerating turbidity current, it is possible that larger and denser taxa (e.g. fern spores) settle out first, while more buoyant (e.g. saccate) pollen taxa settle out later and concentrate at the tops of turbidite beds.

In this study, we analyse changes in pollen distribution within four fine-grained (i.e. silt-rich) turbidites from three sediment cores from the Hikurangi Subduction Margin to ascertain whether differential sorting of taxa occurs during the deposition of fine-grained turbidites (Fig. 1). The Hikurangi Subduction Margin (Lewis and Pettinga, 1993; Wallace et al., 2009), situated offshore the east coast of Aotearoa-New Zealand, is characterised by a network of canyons that incise the continental shelf, with one of the prominent canyons being the Kaikōura Canyon (Fig. 1; Lewis and Barnes, 1999; Mountjoy et al., 2009, 2018; McArthur and McCaffrey, 2019). Canyons on the margin feed sediment into the Hikurangi Channel (~1800 km long, 1.5–12 km wide; Fig. 1), which plays a crucial role in sediment transport along the margin (Lewis et al., 1998; Lewis and Pantin, 2002). Turbidity currents, typically triggered by seismic (Piper and Normark, 2009; Pouderoux et al., 2012a; Mountjoy et al., 2018; Howarth et al., 2021) or storm events (Piper and Normark, 2009; Pouderoux et al., 2012b; Clare et al., 2016), travel down canyons and into the Hikurangi Channel before losing momentum and depositing their sediment as turbidites, both within the Hikurangi Channel and on the overbank lateral to the channel via overspill (Lewis and Pantin, 2002; Tek et al., 2022).

Due to the location of the core sites on the Hikurangi Subduction Margin, we would expect pollen to show regional signals of vegetation, with pollen potentially being sourced from Te Waipounamu-South Island and Te Ika-a-Māui-North Island (Fig. 1). A wide range of vegetation communities can be found in these regions, from native forest (Wardle, 1991; Walker et al., 2006) to exotic forests of primarily *Pinus* introduced during European colonisation in the mid to late 1800s AD (Wilmshurst, 1997; Carter et al., 2002; Elliot et al., 2003; Orpin et al., 2006; Star, 2008; Mildenhall and Orpin, 2010). Several native (McGlone et al., 2017) and introduced conifers (Roche, 1990, 2008) produce saccate pollen (e.g. native podocarps and *Pinus*). Based on this, we expect native podocarp pollen and *Pinus* to be more buoyant than other non-saccate pollen taxa (Tomlinson, 1994; Di-Giovanni et al., 1995; Hirose and Osada, 2016). We also anticipate that robust and larger fern spores like *Cyathea* will be denser than the other pollen taxa (Wilmshurst et al., 1999; McArthur et al., 2016). Therefore, we hypothesise that these denser taxa will be concentrated at the bases of turbidites, while the buoyant pollen types will be concentrated near the tops of turbidites.

## Methods and data set

Turbidites examined for pollen distribution were captured in one high-precision sediment multicore TAN1613-58, and two longer

piston cores TAN1613-47 and TAN1613-46, collected in 2016 AD, by the National Institute of Water and Atmosphere on the RV *Tangaroa* (Fig. 1; Barnes et al., 2017). These cores were chosen to represent both proximal and distal turbidites to the Kaikōura Canyon, and both in-channel and overbank depositional environments (Fig. 1; Table 1). Core TAN1613-58, collected ~145 km from the Kaikōura Canyon head, is the most up-channel site and contains a turbidite deposited by a turbidity current triggered by the 2016 Kaikōura Earthquake (Fig. 1; Table 1; Clark et al., 2017; Hamling et al., 2017; Litchfield et al., 2018; Mountjoy et al., 2018; Howarth et al., 2021; Maier et al., 2024). Cores TAN1613-47 and TAN1613-46 are positioned ~670 km from the head of the Kaikōura Canyon and are located within the Hikurangi Channel and on the NW overbank, respectively (Fig. 1; Table 1; Ganguly, 2018). The turbidites sampled in TAN1613-47 and TAN1613-46 are likely the penultimate turbidites in the sediment cores, and while there is no direct age dating on these turbidites, it is inferred that they were likely deposited in the last ~150 years (Hayward et al., 2022a, 2022b; Maier et al., 2024). In TAN1613-46, this inference is supported by age control deeper in the core from the presence of a primary Taupō tephra at 279.75 cm, which is inferred to have been emplaced in  $232 \pm 10$  AD (Hopkins et al., 2020). Additionally, the presence of exotic pollen like *Pinus* in the turbidites would support this and constrain the age of the deposits to being after European colonisation (Wilmshurst, 1997; Carter et al., 2002; Elliot et al., 2003; Orpin et al., 2006; Mildenhall and Orpin, 2010).

## Core scanning and grain-size analysis

Grain-size measurements were obtained from the selected Hikurangi Subduction Margin turbidites to evaluate the relationship between turbidite facies (Maier et al., 2024) and pollen assemblages. Linescan images and computed tomography (CT; Mees et al., 2003) scans were available for the two piston cores, but only CT scans were available for the short multicore. Raw CT values and scans were processed in ImageJ (National Institutes of Health, 2023), and sediment density was extracted from this data, using the methods of Ashi (1993) and Reilly et al. (2017). The grain size was measured at varying resolutions through the turbidites with a Beckman Coulter LS 13 320 Laser Diffraction Particle Size Analyser, using a quartz model and Mie theory. Grain-size data were processed in MATLAB using the software AnalySize (Paterson and Heslop, 2015) and compiled using Strater (Golden Software, LLC, 2023). The lithofacies scheme of Maier et al. (2024) was used to define facies that make up the turbidite, enhancing our understanding of how the sedimentation changes from the base to the top of the turbidite (Table 2).

## Pollen extraction, counting and analysis

Sediment samples weighing between 5 and 6 g were collected from 1-cm-thick intervals of each turbidite for pollen analysis, with the wet weight of each sample recorded. In total, 29 samples were processed and analysed for pollen (5 samples from TAN1613-58, 14 samples from TAN1613-47 and

**Table 1.** TAN1613 sediment core locations on the Hikurangi Subduction Margin (Fig. 1).

Sample number	Latitude	Longitude	Water depth (m)	Core length (m)	Distance along Hikurangi Channel from Kaikōura Canyon head (km)	Position relative to Hikurangi Channel
TAN1613-58	-42.23283	174.9648	2446	0.62	~145	Channel margin
TAN1613-47	-40.16283	178.93962	3415	3.13	~670	In-Channel
TAN1613-46	-40.1277	178.81183	3219	4.3	~670	Overbank

**Table 2.** Turbidite facies descriptions and process interpretations from Maier et al. (2024).

Facies	Description	Process interpretation	Core examples
$T_d$	Planar-laminated silt and fine to very fine sand	Direct suspension sedimentation with traction or near-bed effects	All cores
$T_{e1}$	Laminated silt-rich mud; may contain layering or pulses	Direct suspension sedimentation at the tail end of the turbidity current and its collapse with near-bed effects	TAN1613-58
$T_{e2}$	Normally graded silt-rich mud	Direct suspension sedimentation at the tail end of the turbidity current and its collapse	TAN1613-47; 46
$T_{e3}$	Homogeneous silt-rich mud	Direct suspension sedimentation or cohesive transitional flow at the end of turbidity current runout and collapse	TAN1613-47

10 samples from TAN1613-46). *Lycopodium clavatum* tablets (Stockmarr, 1971) were added as a pollen-counting standard to allow the calculation of pollen concentration. The samples were reacted with 10% hydrochloric acid to remove carbonates. Standard pollen extraction methods (Faegri et al., 1989) were followed, including removing humic acid with a 1:1 ratio of potassium hydroxide and sodium pyrophosphate, sieving through a 6  $\mu\text{m}$  mesh, separating the organics from the bulk material with sodium polytungstate (specific gravity = 2–2.1  $\text{g}/\text{cm}^3$ ; Campbell et al., 2016; van den Bos et al., 2020), acetolysis (9:2 mixture of acetic anhydride and concentrated sulphuric acid), alcohol dehydration (tertiary butyl alcohol) and mounting in silicon oil. Both pollen (i.e. from Angiosperms and Gymnosperms) and spores (i.e. Pteridophytes) were counted and included in totals and calculations of pollen concentration. Pollen grains were identified using key texts (Pocknall, 1981a, 1981b, 1981c; Large and Braggins, 1991; Moar, 1993) and counted using a PolyCounter (Nakagawa, 2007). For each sample, where possible, >250 pollen grains were counted, excluding *L. clavatum*. The concentration of pollen in each sample was calculated according to Stockmarr (1971). Pollen data were plotted in Tilia (Grimm, 2020). One-way analysis of variance (ANOVA) was conducted in R (R Core Team, 2021) on the percentage of pollen taxa in each turbidite, with coding assistance from ChatGPT (2023). Additionally, multivariate analysis of variance (MANOVA) was conducted on the pollen group percentages in the turbidite in TAN1613-47. MANOVA was not conducted on the pollen group percentages in TAN1613-58 and TAN1613-46 because the number of samples in these turbidites was less than the number of pollen groups (the number of observations was less than the number of dependent variables; Krzanowski, 2000).

## Results

### TAN1613-58

In core TAN1613-58, we targeted the uppermost turbidite from 8 to 0 cm below the seafloor (cbsf), which was deposited as a result of the 2016 Kaikōura Earthquake (Figs. 1 and 2A; Maier et al., 2024; Mountjoy et al., 2009). The base of the turbidite (~7.5–6 cbsf) consists of planar laminated coarse-silt with some very-fine-sand (Facies  $T_d$ ), normally grading to laminated medium-to-fine-silt at ~5 cbsf (Facies  $T_{e1}$ , Fig. 2A). The bed is coarsest (very-fine-sand) at 6.75 cbsf, where the sediment is 55% sand, 43.5% silt and <1.5% clay (Fig. 2A). At 5.25 cbsf, the percentage of sand decreases significantly to 5%, and silt and clay both increase to 77% and 18%, respectively (Fig. 2A). Above 4 cbsf, the sediment normally grades to fine-silt, with the proportions of sand (0–2%), silt (79–84%) and clay (9–12%) remaining relatively steady (Fig. 2A). There are three thin laminae above the base of the turbidite that are represented by density peaks at 5, 4.6 and 3.7 cbsf (Facies  $T_d$ ).

In the five pollen samples analysed, the upper four samples are from the most recent turbidite, with the sample at 8.5 cbsf retrieved from the underlying bed, which is likely either hemipelagite or the top of a previous turbidite (Fig. 2A; Barnes et al., 2017). Ferns and fern allies are found in high percentages through the bed with *Pteridium* being the most abundant (Figs. 2 and 3A). Exotic *Pinus* pollen is also very abundant throughout the bed, with the majority of this interpreted to be *Pinus radiata*, due to its prevalence in onshore forestry (Figs. 2 and 3A, Allen and Lee, 2006; Roche, 1990, 2008). Of the podocarps *Dacrydium cupressinum* and *Prumnopitys taxifolia* are the most abundant (Figs. 2 and 3A). The beech pollen, *Fuscospora* sp., appears consistently throughout the turbidite, as does grass pollen (Poaceae, Figs. 2 and 3A). As a group, small trees and shrubs make up the lowest percentage of all the pollen groups (Figs. 2 and 3A). The sample from below the turbidite at 8.5 cbsf does not largely differ in its overall pollen assemblage from the four samples from within the upper turbidite (Figs. 2 and 3A). ANOVA shows that the proportions of individual taxa do not vary significantly within the four samples from the turbidite (all taxa  $p > 0.05$ ; Figs. 2 and 3A). However, pollen concentration varies significantly (d.f. = 1,  $F = 28.69$ ,  $p = 0.03313$ ), with the lowest concentration at the base of the bed, increasing towards the top of the turbidite (Figs. 2 and 3A). Overall, pollen concentration is the highest in the sample from below the turbidite (8.5 cbsf, 7165 grains/g), followed by the uppermost sample (0.5 cbsf, 6698 grains/g), interpreted as the turbidite tail (Figs. 2 and 3A).

### TAN1613-47

In core TAN1613-47, we sampled the penultimate turbidite from 124 to 37 cbsf (Figs. 1 and 2B). The silt content is consistently high through this turbidite, ranging between 74% and 90% (Fig. 2B). The turbidite has a coarse-silt base, with 19.5% sand, 77% silt and 3% clay (Fig. 2B). The interval from the base to 78 cbsf normally grades to medium-silt and has planar laminations (Facies  $T_d$ , Fig. 2B). In this same interval, clay content gradually increases to 20% at 78 cbsf, and sand content decreases to 0% (Fig. 2B). From 78 to 72 cbsf, the sediment normally grades to very-fine-silt (Facies  $T_{e2}$ ) and remains relatively homogeneous from 72 to 37 cbsf (Facies  $T_{e3}$ , Fig. 2B).

Spores from ferns and fern allies dominate the spectra in the TAN1613-47 turbidite, with *Pteridium* and *Cyathea* making up the majority of this group (Figs. 2 and 3B). Podocarps and hardwoods are the second most represented group, with abundant *D. cupressinum*, *P. taxifolia* and *Prumnopitys ferruginea* (Figs. 2 and 3B). Pollen from the groups beech, small trees and shrubs, herbs and grasses appear consistently through the bed (Figs. 2 and 3B). There is a minor amount of exotic taxa in the bed, including *Pinus* (<2.7%) and Chenopodiaceae (Figs. 2 and 3B). ANOVA shows that the proportions of individual taxa do not

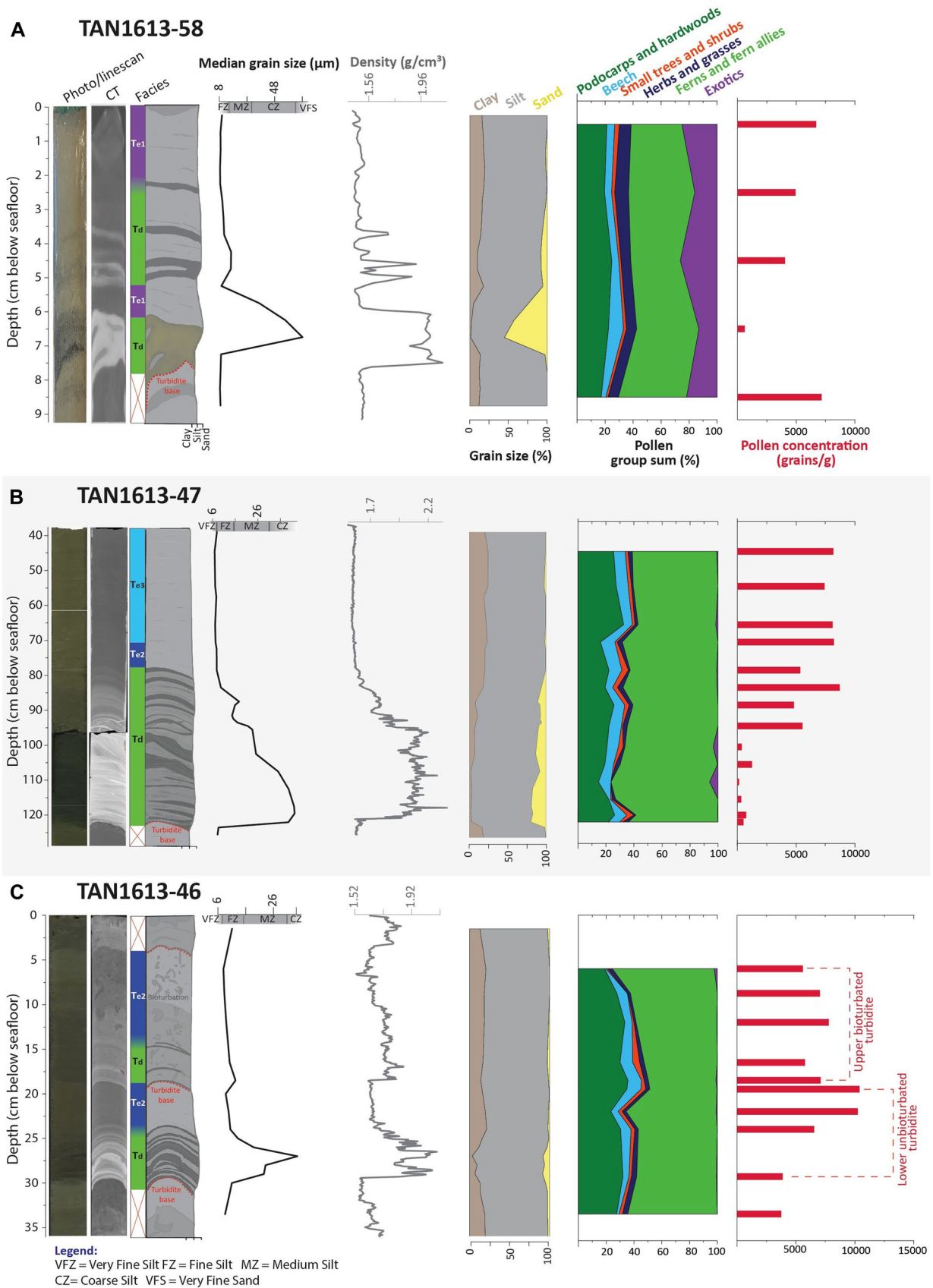


**Figure 2.** Sedimentology and palynology data for (A) TAN1613-58, (B) TAN1613-47 and (C) TAN1613-46. Group headings and axes labels in plot A apply to plots B and C. Refer to Table 2 for descriptions of turbidite facies (Maier et al., 2024). [Color figure can be viewed at wileyonlinelibrary.com]

vary significantly between the samples in the turbidite (all taxa  $p > 0.05$ ). Results from MANOVA support this, as the pollen group assemblage does not vary significantly between the samples in the turbidite (Pillai's trace = 0.3042,  $F(6, 7) = 0.5100$ ,  $p = 0.7850$ ). However, the pollen concentration does

vary significantly between the samples (d.f. = 1,  $F = 42.70$ ,  $p = 2.792 \times 10^{-5}$ , Figs. 2 and 3B). The pollen concentrations are very low (<1500 grains/g) in the lower 20 cm of the turbidite and sharply increase to between 4813 and 8700 grains/g in the upper, medium-to-fine-silt portion of the turbidite (Fig. 2B).

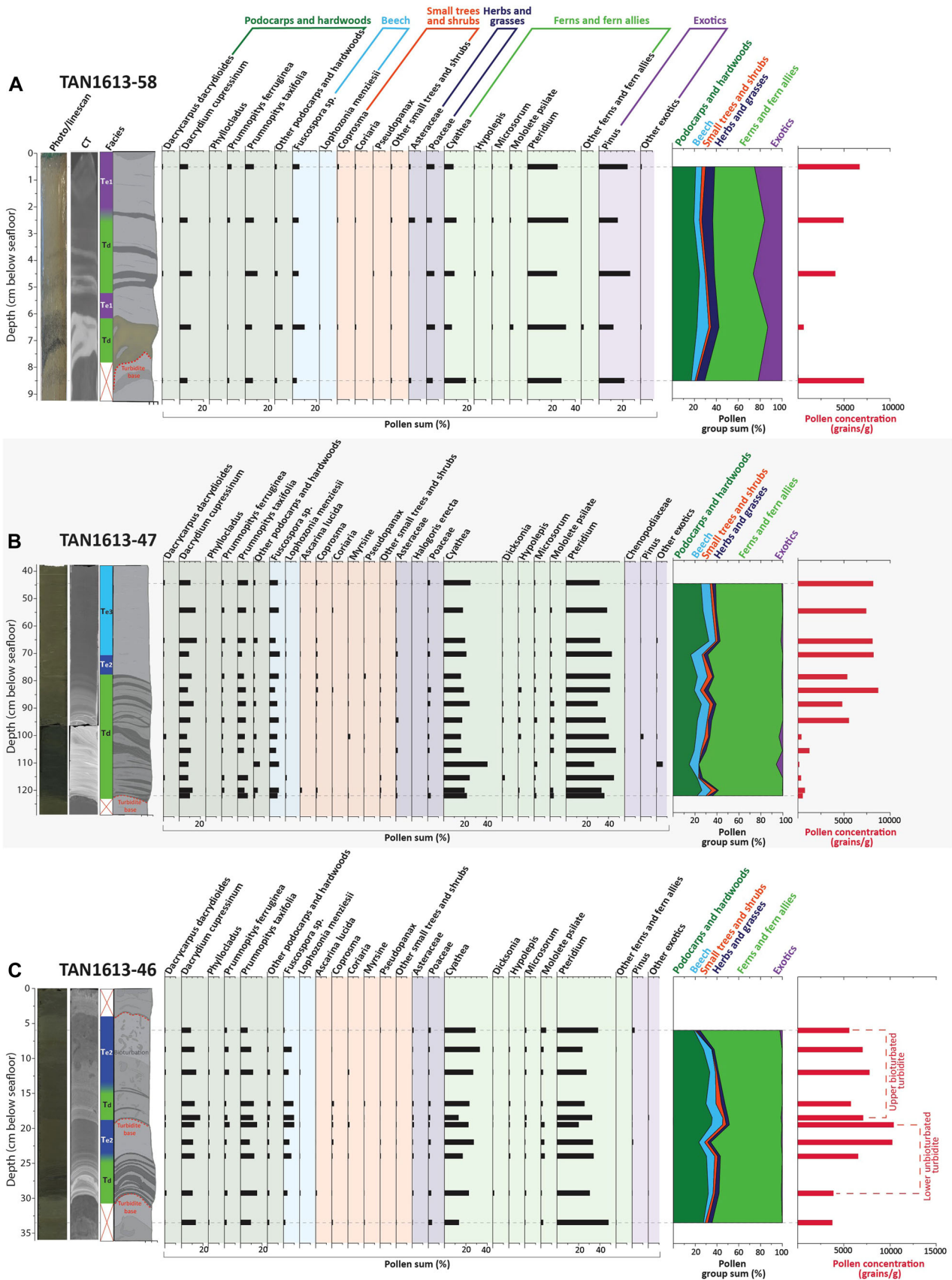


**Figure 3.** Expanded pollen data for (A) TAN1613-58, (B) TAN1613-47 and (C) TAN1613-46. The ‘other’ categories are for pollen taxa with counts below five or where identification was uncertain. Refer to Table 2 for descriptions of turbidite facies (Maier et al., 2024). [Color figure can be viewed at [wileyonlinelibrary.com](https://onlinelibrary.wiley.com)]

**TAN1613-46**

In core TAN1613-46, we sampled two turbidites: a ‘lower-turbidite’ from 29.8 to 18.5 cmbsf and the overlying ‘upper-

turbidite’ from 18.5 to 4 cmbsf (Figs. 1 and 2C). Overall, both of the turbidites have a high silt content (78–88%), moderate clay content (up to 21%) and low sand content (<8%, Fig. 2C). The lower turbidite has a medium-to-coarse-silt base with

planar laminations to ~24 cmbsf (Facies  $T_d$ ), above which the sediment normally grades to fine-silt until the top of the bed at 18.5 cmbsf (Facies  $T_{e2}$ , Fig. 2). The base of the upper turbidite at 18.5 cmbsf is marked by small peaks in grain-size and density (Facies  $T_d$ , Fig. 2C). From 15 to 4 cmbsf, the sediment normally grades, with some minor peaks in density (Facies  $T_{e2}$ , Fig. 2C). The upper bed is bioturbated, with the degree of bioturbation being the highest in Facies  $T_{e2}$  (Fig. 2C). The upper turbidite is dominated by silt, with the ratio of sand (<3%), silt (80–84%) and clay (14–18%) staying relatively consistent through the bed (Fig. 2C).

Ferns and fern allies are the most abundant pollen group in TAN1613-46, with high percentages of both *Pteridium* and *Cyathea* (Figs. 2 and 3C). Podocarps and hardwoods are also abundant throughout the bed, with the consistent appearance of *D. cupressinum*, *P. taxifolia*, *P. ferruginea*, and in smaller amounts *Phyllocladus* and *Dacrycarpus dacrydioides* (Figs. 2 and 3C). The beech taxa, *Fuscospora* sp., appears consistently through both beds, as does Asteraceae and Poaceae in smaller amounts (Figs. 2 and 3C). Small trees and shrubs comprise the lowest portion of all the pollen groups in TAN1613-46, but there is still a consistent presence of taxa like *Coprosma* and *Coriaria* throughout the beds (Figs. 2 and 3C). There is a minor amount of the exotic taxa *Pinus* in both beds (<2.5%, Figs. 2 and 3C). In the lower turbidite, the percentage of taxa between samples does not vary significantly (all taxa  $p > 0.05$ ), but pollen concentration does vary significantly (d.f. = 1,  $F = 20.01$ ,  $p = 0.04652$ ), with the lowest values (3754–3875 grains/g) at the base of the turbidite, increasing to 10,408 grains/g at the top of the turbidite (Figs. 2 and 3C). In the upper turbidite, the percentage of individual taxa does not vary significantly between samples (all taxa  $p > 0.05$ ), and neither does pollen concentration (d.f. = 1,  $F = 0.1330$ ,  $p = 0.7396$ ), which varies between 5595 and 7798 grains/g through the entire turbidite (Figs. 2 and 3C).

## Discussion

Sampling of fine-grained turbidites from the Hikurangi Subduction Margin reveals that a wide range of pollen taxa can be found in these deep marine deposits (Figs. 2 and 3; Table 3). Overall, 41 taxa were confidently identified across the three sediment cores (Table 3), including most of the major native forest taxa that we would expect in sediments offshore the northern east coast of Aotearoa from the past 150 years (Figs. 2 and 3; Carter et al., 2002; Crouch et al., 2010; Elliot et al., 2003; Mildenhall and Orpin, 2010; Orpin et al., 2006; Wilmschurst, 1997). Ferns and fern allies dominate the TAN1613 cores, making up 57.9% of the total pollen (Table 3). Of the ferns and fern allies, *Pteridium* was the most abundant (33.6% of the total pollen), followed by *Cyathea* (19.6% of the total pollen, Fig. 3; Table 3). Podocarps and hardwoods comprise the second-highest percentage of the pollen groups, accounting for 25.1% of the total pollen (Table 3). Of this group, *D. cupressinum* contributes 11.2% of the total pollen and

*P. taxifolia* contributes 8.8%, while the other eight groups contribute smaller percentages (each less than 2.2%, Table 3). Small trees and shrubs make up the lowest percentage of the total pollen (2.6%), with *Coprosma* making up the highest proportion (0.9%) of this group (Table 3).

Pollen concentration varied significantly between the bases and the tops of the TAN1613 turbidites, with the exception of the bioturbated upper turbidite in TAN1613-46 (Fig. 2). Pollen concentration was generally lowest in the coarser basal turbidite layers (Facies  $T_d$ ), with the lowest observed concentration being 157 grains/g in the base of TAN1613-47 (Figs. 2 and 3). In the finer upper portions of the turbidites, in the  $T_{e1}$  and  $T_{e2}$  Facies, pollen concentration was significantly higher, reaching as high as 10,407 grains/g in TAN1613-46 (Figs. 2 and 3). This clearly shows that as the sediment normally grades to fine-silt in the  $T_{e1}$  and  $T_{e2}$  Facies, pollen concentration increases (Fig. 2). This trend of increasing pollen concentration as the sediment fines is similar to what was observed in Porro (2018) but in coarser sand-silt turbidites.

Due to the varied shapes, sizes and densities of pollen grains (Di-Giovanni et al., 1995; Hirose and Osada, 2016; Holmes, 1990), we expected to see some sorting of pollen in the TAN1613 turbidites. We anticipated that denser taxa (e.g. *Cyathea*) would drop out of the turbidity current first, followed by more buoyant taxa (e.g. *Pinus*) when the turbidity current began to lose momentum. This process would facilitate the sorting of pollen taxa similarly to how other grains are sorted in turbidity currents (Stow and Bowen, 1980; Talling et al., 2012). The TAN1613-58 turbidite, deposited by a turbidity current triggered by the 2016 Kaikōura Earthquake (Mountjoy et al., 2018; Howarth et al., 2021), contains abundant *Pinus* pollen, reflecting the prevalence of modern onshore forestry (Fig. 3A; Roche, 1990, 2008; Allen and Lee, 2006; Crouch et al., 2010). Contrary to our hypothesis, *Pinus* pollen was found throughout the turbidite in similar proportions when compared to the total pollen assemblage (Fig. 3A). The turbidites in TAN1613-47 and TAN1613-46 had minor amounts of *Pinus* pollen, supporting the hypothesis that they were deposited in the last 150 years, likely shortly after European colonisation (Fig. 3B, C; Wilmschurst, 1997; Carter et al., 2002; Elliot et al., 2003; Orpin et al., 2006; Mildenhall and Orpin, 2010). Although these turbidites had lower levels of exotic pollen than TAN1613-58, even in small quantities *Pinus* did not vary significantly through these turbidites (Figs. 2 and 3). Other saccate pollen (e.g. native Podocarps) likewise showed a similar trend to *Pinus*, appearing throughout each turbidite in consistent percentages (Figs. 2 and 3). Additionally, although fern spores like *Cyathea* are relatively large and dense, these grains showed no evidence of sorting and were not concentrated at the bases of turbidites as we hypothesised (Fig. 3). Furthermore, other non-saccate pollen (e.g. small trees and shrubs, herbs and grasses) also did not vary significantly between samples in each of the turbidites (Fig. 3). Hence, we can conclude that pollen is not differentially sorted due to size, shape or density in fine-grained turbidites on the Hikurangi Subduction Margin (Fig. 4). This finding is intriguing given the varying distance of each core along the Hikurangi Channel and the differing positions of each core relative to the channel (i.e. in-channel or overbank; Fig. 1; Table 1). Furthermore, each turbidite had variable thicknesses and sedimentary features (e.g. TAN1613-58 turbidite = 8 cm thick, TAN1613-47 turbidite = 87 cm thick; Fig. 2), highlighting the significance of the observed consistency in pollen trends.

The pollen distribution observed in the TAN1613 turbidites can potentially shed light on turbidity current processes on the Hikurangi Subduction Margin (Fig. 4). The diluted volume of pollen at the bases of the turbidites (Fig. 2) shows that pollen was

**Table 3.** Summary of pollen groups found across the three TAN1613 cores.

Pollen group	Percentage of total pollen	Number of taxa identified
Podocarps and hardwoods	25.1	10
Beech	6.8	2
Small trees and shrubs	2.6	11
Herbs and grasses	3.6	3
Ferns and fern allies	57.9	8
Exotics	4	7

not preferentially deposited when the coarser grains dropped out of the turbidity current (Fig. 4). It is plausible that the pollen largely bypassed this first coarser-grained depositional phase of the turbidity current and was instead concentrated in an upper, finer-grained layer of the turbidity current (Fig. 4). Then as the turbidity current lost momentum, the finer sediment and the bulk of the pollen would have been deposited, resulting in the observed increase in pollen concentration in the turbidite tails (Fig. 2). However, the relative proportions of pollen taxa remain fairly consistent within each turbidite sampled in the TAN1613 cores (Fig. 3). This uniformity implies that the formative turbidity currents may not have been entirely turbulent, instead exhibiting transitional flow behaviours (Baas et al., 2009, 2011; Talling, 2013). The substantial silt and clay content (as high as 90% and 24%, respectively) would have increased cohesion in the flow, resulting in modulated turbulence in the turbidity current (Fig. 2; McCave and Jones, 1988; Baas et al., 2009; Talling, 2013). Put simply, the turbidity currents that deposited the TAN1613 turbidites were not sufficiently turbulent to sort the pollen taxa according to their size, shape or density (Fig. 4). In contrast, in a less dense and highly turbulent flow scenario (Talling et al., 2012), we could potentially expect to observe sorting of pollen taxa, with buoyant, saccate taxa concentrated at the tops of turbidites. A more turbulent flow scenario like this could occur further along the Hikurangi Channel after the coarser sediment has been deposited and only fine sediment remains in suspension. For example, Maier et al., 2024 identified a thin turbidite deposited from the 2016 Kaikōura Earthquake, ~1300 km from the Kaikōura Canyon in the Hikurangi Fan Drift (Lewis, 1994). This deposit was entirely  $T_{e3}$  Facies, and in a deposit such as this, we cannot rule out the possibility of pollen taxa being sorted.

An important implication from a palaeovegetation perspective is that, with the exception of some of the rarer taxa, the pollen spectra from any given sample depth in a turbidite would yield the same palaeovegetation interpretation (Fig. 4). Hence, we suggest that fine-grained turbidites can be sampled for pollen for the purpose of creating palaeovegetation records. Despite this, care should still be taken when using pollen spectra changes in a turbiditic record to infer changes in past onshore vegetation. It has been established that pollen assemblages recovered from marine records, particularly distal records, have inherent biases from differential transport and preservation of certain pollen grains (McGlone, 2001; Mildenhall, 2003; Crouch et al., 2010). Inter-

estingly, the TAN1613 turbidite pollen assemblages show similar trends to what has been observed in other records from offshore the east coast of Aotearoa. Notably, the TAN1613 turbidites have an over-representation of robust fern spores and high levels of hydrodynamically efficient saccate podocarp pollen (Table 3), as was also found in the cores P69 (McGlone, 2001), W369 (Wilmshurst et al., 1999), ODP-1123 (Mildenhall, 2003) and in surface sediment samples from offshore eastern Aotearoa (Crouch et al., 2010; Fig. 1). In this way, it appears that the TAN1613 turbidites preserve a pollen signal that is not dissimilar to sedimentary records that are mostly background sedimentation. A complication of sampling pollen in turbidites for palaeovegetation reconstructions is that deposits could potentially contain reworked pollen from along the path of the turbidity current (Talling et al., 2012; Pope et al., 2022). However, even in non-turbiditic sediments, there is potential for reworked grains from both terrestrial and marine environments. For example, Wilmshurst et al. (1999) noted the presence of Tertiary pollen reworked from onshore soils in core W369, from Poverty Bay (Fig. 1). Therefore, we suggest that the same care should be taken when interpreting palaeovegetation records from turbidites as in any marine sedimentary record. Depending on the core location, in some instances, it could be argued that pollen from turbidites in a deep marine core could provide a more complete record of past vegetation than pollen from background sediments. For example, it is plausible that turbidity currents sourced from canyon systems that are closely coupled to river mouths could eliminate biases that occur as a result of the long transport path of pollen that slowly settles with background sedimentation, as stated in Mildenhall (2003). This is supported by the findings of Jolley et al. (2022) that the pollen assemblages in turbidites from the North Sea Basin closely resemble the terrestrial vegetation at the sediment source area. To validate the accuracy of palaeovegetation records obtained from turbidites, a longer vegetation record covering multiple climatic shifts through the sampling of pollen in turbidite sequences would need to be reconstructed. Such a turbidite pollen record could then be compared to pollen assemblages from other nearby marine pollen records, to quantitatively assess the similarities and differences in the pollen assemblages.

### Guide to sampling pollen in fine-grained turbidites

Pollen results from the Hikurangi Subduction Margin turbidites indicate that for palaeovegetation reconstructions, a pollen

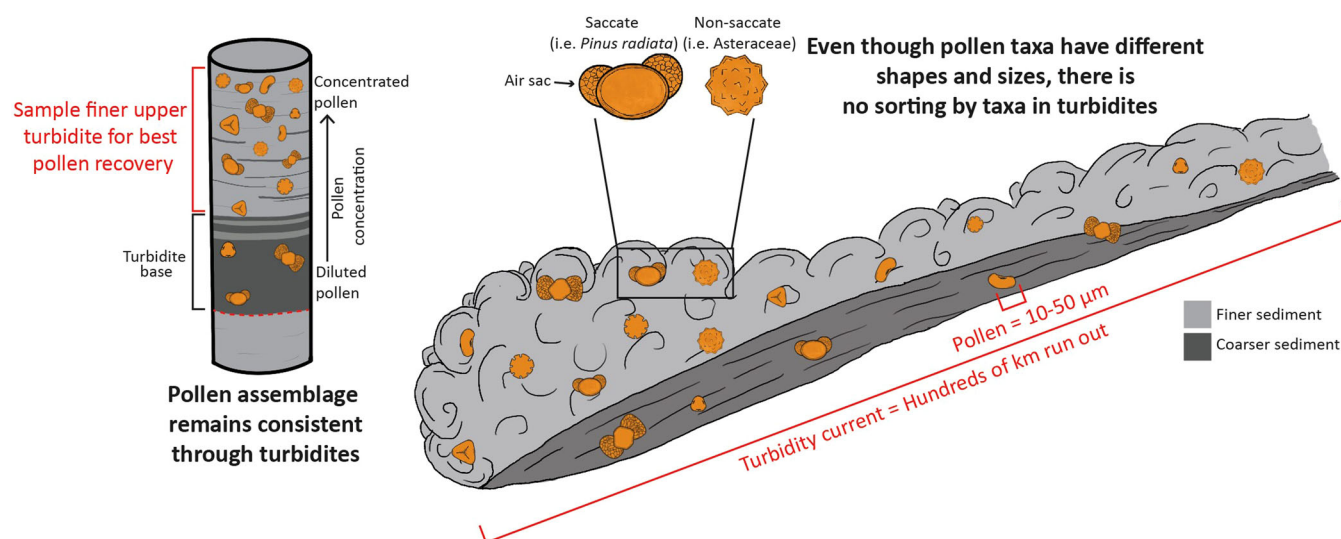


**Figure 4.** Summary schematic of findings that pollen (not to scale) is not sorted by taxa in fine-grained turbidites on the Hikurangi Subduction Margin, and that sampling the upper finest part of a turbidite will give the best pollen recovery. [Color figure can be viewed at [wileyonlinelibrary.com](https://onlinelibrary.wiley.com/doi/10.1002/jqs.3653)]

sample could be taken from any interval in a fine-grained (i.e. silt-rich) turbidite and be assumed to represent the pollen spectra of the whole turbidite (Fig. 4). However, to get the highest pollen recovery, it is best to avoid sampling the basal layer of a turbidite and instead sample where the sediment begins to fine, as our results show that pollen is diluted in the coarser basal layers of turbidites (Fig. 4). Although pollen taxa were not sorted in these fine-grained turbidites, this does not rule out the possibility of sorting by taxa in other types of turbidites (e.g. coarser-grained sand-silt turbidites). Therefore, we recommend that before sampling a turbidite for pollen, take a sample from the basal and upper part of the turbidite to check that the pollen assemblage is consistent.

## Conclusion

Pollen analysis of Hikurangi Subduction Margin turbidites indicates that in fine-grained (i.e. silt-rich) turbidites, sampling at any depth within a turbidite will yield a similar pollen assemblage. This is beneficial for vegetation reconstructions as this means that the spectra of a single pollen sample from a turbidite will be representative of the pollen assemblage in the whole turbidite. Therefore, this demonstrates that fine-grained turbidites are suitable for pollen sampling for reconstructions of regional onshore vegetation. This is significant for active margins, like the Hikurangi Subduction Margin where many sedimentary records are dominated by turbidites, as these findings show that turbidites in these cores can be sampled for pollen to create records of past vegetation. Although pollen taxa were not sorted in the fine-grained TAN1613 turbidites, this does not rule out the possibility of sorting by taxa in other types of turbidites (e.g. sand-rich turbidites). In fine-grained turbidites, we suggest sampling the tails of turbidites to get the highest pollen recovery. We propose that fine-grained turbidites can provide good pollen recovery and offer an untapped opportunity to determine long-term vegetation changes on active margins.

**Acknowledgements.** We acknowledge and thank the National Institute of Water and Atmospheric Research (NIWA), Taihoro Nukurangi, for the use of the TAN1613 cores and their facilities for core sampling and analyses. Thank you to Grace Frontin-Rollet from NIWA for help with sampling, grain-size analysis and carbonate analysis. We also thank Massey University, Palmerston North, for the use of the palynology laboratory. Open access publishing facilitated by The University of Auckland, as part of the Wiley - The University of Auckland agreement via the Council of Australian University Librarians.

## Data availability statement

The data that support the findings of this study are openly available on Zenodo at <https://zenodo.org/doi/10.5281/zenodo.12753120>.

**Abbreviations.** ANOVA, analysis of variance; cmbst, centimetres below the seafloor; CT, computed tomography; CZ, coarse silt; dUC, D'Urville current; EAUC, East Auckland current; ECC, East Cape current; FZ, fine silt; MANOVA, multivariate analysis of variance; MZ, medium silt; NIWA, National Institute of Water and Atmospheric Research; ODP, Ocean Drilling Program; VFS, very fine sand; VFZ, very fine silt; WCC, Wairarapa Coastal current.

## References

Allen, R.B. & Lee, W.G. (2006) *Biological invasions in New Zealand*, vol. 186. Springer Science & Business Media.  
 Ashi J. (1993) CT scan analysis of sediments from LEG 1461. In: *Proceedings of the Ocean Drilling Program, Scientific Results*, ch 11, 146 vol. Ocean Drilling Program.

Baas, J.H., Best, J.L. & Peakall, J. (2011) Depositional processes, bedform development and hybrid bed formation in rapidly decelerated cohesive (mud-sand) sediment flows. *Sedimentology*, 58(7), 1953–1987.  
 Baas, J.H., Best, J.L., Peakall, J. & Wang, M. (2009) A phase diagram for turbulent, transitional, and laminar clay suspension flows. *Journal of Sedimentary Research*, 79(4), 162–183.  
 Barnes P.M., Orpin A., Howarth J., Patton J.R., Lamarche G., Woelz S., et al. (2017) *Using sedimentary core records to unravel the earthquake history of the Hikurangi Subduction Zone*. Tangaroa TAN1613 voyage report. National Institute of Water and Atmospheric Research Ltd.  
 Beaudouin, C., Dennielou, B., Melki, T., Guichard, F., Kallel, N., Berné, S. et al. (2004) The Late-Quaternary climatic signal recorded in a deep-sea turbiditic levee (Rhône Neofan, Gulf of Lions, NW Mediterranean): palynological constraints. *Sedimentary Geology*, 172(1–2), 85–97.  
 Campbell, J., Fletcher, W., Hughes, P. & Shuttleworth, E. (2016) A comparison of pollen extraction methods confirms dense-media separation as a reliable method of pollen preparation. *Journal of Quaternary Science*, 31(6), 631–640.  
 Carter, L., Manighetti, B., Elliot, M., Trustrum, N. & Gomez, B. (2002) Source, sea level and circulation effects on the sediment flux to the deep ocean over the past 15 ka off eastern New Zealand. *Global and Planetary Change*, 33(3–4), 339–355.  
 ChatGPT (2023) *Code assistance with R programming*. OpenAI Forum. <https://forum.openai.com>  
 Clare, M.A., Clarke, J.H., Talling, P.J., Cartigny, M.J. & Pratomo, D. (2016) Preconditioning and triggering of offshore slope failures and turbidity currents revealed by most detailed monitoring yet at a fjord-head delta. *Earth and Planetary Science Letters*, 450, 208–220.  
 Clark, K., Nissen, E., Howarth, J., Hamling, I., Mountjoy, J., Ries, W. et al. (2017) Highly variable coastal deformation in the 2016 Mw7.8 Kaikōura earthquake reflects rupture complexity along a transpressional plate boundary. *Earth and Planetary Science Letters*, 474, 334–344.  
 Crouch, E., Mildenhall, D. & Neil, H. (2010) Distribution of organic-walled marine and terrestrial palynomorphs in surface sediments, offshore eastern New Zealand. *Marine Geology*, 270(1–4), 235–256.  
 Di-Giovanni, F., Kevan, P. & Nasr, M. (1995) The variability in settling velocities of some pollen and spores. *Grana*, 34(1), 39–44.  
 Elliot, M., Manighetti, B. & Carter, L. (2003) In the beginning—high resolution evidence from a deep ocean core for the early settlement of New Zealand. In: Gao, J., LeHeron, R. & Logie, J. (Eds.) *Windows on a changing world. Proceedings of the 22nd New Zealand Geographical Society Conference, New Zealand Geographical Society Conference Series*. pp. 92–96.  
 Faegri K., Iversen J., Kaland P.E., Krzywinski K. (1989) *Textbook of pollen analysis*. 4th edition. John Wiley & Sons Ltd.  
 Ganguly, A. (2018) Sediment deposits in the Hikurangi Channel and links to seismic activity. Masters Thesis.  
 Golden Software, LLC (2023) Strater 5.  
 Grimm, E.C. (2020) Tilia. Version 3.0.1.  
 Gutiérrez-Pastor, J., Nelson, C.H., Goldfinger, C. & Escutia, C. (2013) Sedimentology of seismo-turbidites off the Cascadia and northern California active tectonic continental margins, northwest Pacific Ocean. *Marine Geology*, 336, 99–119.  
 Hamling, I.J., Hreinsdóttir, S., Clark, K., Elliott, J., Liang, C., Fielding, E. et al. (2017) Complex multifault rupture during the 2016 Mw 7.8 Kaikōura earthquake, New Zealand. *Science*, 356(6334), eaam7194.  
 Harris, P.T. & Whiteway, T. (2011) Global distribution of large submarine canyons: geomorphic differences between active and passive continental margins. *Marine Geology*, 285(1–4), 69–86.  
 Hayward, B.W., Sabaa, A.T., Howarth, J.D., Orpin, A.R. & Strachan, L.J. (2022a) Foraminiferal evidence for the provenance and flow history of turbidity currents triggered by the 2016 Kaikōura Earthquake, New Zealand. *New Zealand Journal of Geology and Geophysics*, 67(3), 336–349.  
 Hayward, B.W., Sabaa, A.T., Howarth, J.D., Orpin, A.R., Strachan, L.J. & Tickle, S.E. (2022b) Foraminiferal insights into the complexities of the turbidity currents triggered by the 2016 Kaikōura Earthquake, New Zealand. *Marine Micropaleontology*, 176, 102171.  
 Heusser, L. & Balsam, W.L. (1977) Pollen distribution in the northeast Pacific Ocean. *Quaternary Research*, 7(1), 45–62.  
 Hirose, Y. & Osada, K. (2016) Terminal settling velocity and physical properties of pollen grains in still air. *Aerobiologia*, 32, 385–394.

- Holmes, P.L. (1990) Differential transport of spores and pollen: a laboratory study. *Review of Palaeobotany and Palynology*, 64(1-4), 289–296.
- Hopkins, J.L., Wysoczanski, R.J., Orpin, A.R., Howarth, J.D., Strachan, L.J., Lunenburg, R. et al. (2020) Deposition and preservation of tephra in marine sediments at the active Hikurangi subduction margin. *Quaternary Science Reviews*, 247, 106500.
- Howarth, J.D., Orpin, A.R., Kaneko, Y., Strachan, L.J., Nodder, S.D., Mountjoy, J.J. et al. (2021) Calibrating the marine turbidite palaeoseismometer using the 2016 Kaikōura earthquake. *Nature Geoscience*, 14(3), 161–167.
- Jolley, D., Vieira, M., Jin, S. & Kemp, D.B. (2022) Palynofloras, palaeoenvironmental change and the inception of the Paleocene Eocene Thermal Maximum; the record of the Forties Fan, Sele Formation, North Sea Basin. *Journal of the Geological Society*, 180(1), jgs2021–131.
- Krzyszowski W. (2000) *Principles of multivariate analysis*, vol. 23. Oxford: OUP.
- Large M.F., Braggins J.E. (1991) *Spore atlas of New Zealand ferns & fern allies*. Sir Pub.
- Lewis, K. (1994) The 1500-km-long Hikurangi Channel: trench-axis channel that escapes its trench, crosses a plateau, and feeds a fan drift. *Geo-Marine Letters*, 14, 19–28.
- Lewis, K. & Pettinga, J. (1993) The emerging, imbricate frontal wedge of the Hikurangi Margin. *Sedimentary Basins of the World*, 2, 225–250.
- Lewis, K.B. & Barnes, P.M. (1999) Kaikōura Canyon, New Zealand: active conduit from near-shore sediment zones to trench-axis channel. *Marine Geology*, 162(1), 39–69.
- Lewis, K.B., Collot, J.Y. & Lallem, S.E. (1998) The dammed Hikurangi Trough: a channel-fed trench blocked by subducting seamounts and their wake avalanches (New Zealand-France GeodyNZ Project). *Basin Research*, 10(4), 441–468.
- Lewis, K.B. & Pantin, H.M. (2002) Channel-axis, overbank and drift sediment waves in the southern Hikurangi Trough, New Zealand. *Marine Geology*, 192(1-3), 123–151.
- Litchfield, N.J., Villamor, P., Dissen, R.J.V., Nicol, A., Barnes, P.M., A.Barrell, D.J. et al. (2018) Surface rupture of multiple crustal faults in the 2016 Mw 7.8 Kaikōura, New Zealand, Earthquake. *Bulletin of the Seismological Society of America*, 108(3B), 1496–1520.
- Maier, K., Strachan, L., Tickle, S., Orpin, A., Nodder, S. & Howarth, J. (2024) Testing turbidite conceptual models with the 2016 Mw7.8 Kaikōura Earthquake co-seismic event bed, Aotearoa New Zealand. *Journal of Sedimentary Research*, 94(3), 325–333.
- McArthur, A., Gamberi, F., Kneller, B., Wakefield, M., Souza, P. & Kuchle, J. (2017) Palynofacies classification of submarine fan depositional environments: outcrop examples from the Marnoso-Arenacea Formation, Italy. *Marine and Petroleum Geology*, 88, 181–199.
- McArthur, A., Kneller, B., Souza, P. & Kuchle, J. (2016) Characterization of deep-marine channel-levee complex architecture with palynofacies: an outcrop example from the Rosario Formation, Baja California, Mexico. *Marine and Petroleum Geology*, 73, 157–173.
- McArthur, A.D. & McCaffrey, W.D. (2019) Sedimentary architecture of detached deep-marine canyons: examples from the East Coast Basin of New Zealand. *Sedimentology*, 66(3), 1067–1101.
- McCave, I. & Jones, K. (1988) Deposition of ungraded muds from high-density non-turbulent turbidity currents. *Nature*, 333(6170), 250–252.
- McGann, M. (2018) Selective transport of palynomorphs in marine turbiditic deposits: an example from the Ascension-Monterey Canyon system offshore central California. *Quaternary International*, 469, 120–140.
- McGlone, M.S. (2001) A late Quaternary pollen record from marine core P69, southeastern North Island, New Zealand. *New Zealand Journal of Geology and Geophysics*, 44(1), 69–77.
- McGlone, M.S., Richardson, S.J., Burge, O.R., Perry, G.L. & Wilmshurst, J.M. (2017) Palynology and the ecology of the New Zealand conifers. *Frontiers in Earth Science*, 5, 94.
- Mees, F., Swennen, R., Geet, M.V. & Jacobs, P. (2003) Applications of X-ray computed tomography in the geosciences. *Geological Society, London, Special Publications*, 215(1), 1–6.
- Mildenhall, D. (2003) Deep-sea record of Pliocene and Pleistocene terrestrial palynomorphs from offshore eastern New Zealand (ODP Site 1123, Leg 181). *New Zealand Journal of Geology and Geophysics*, 46(3), 343–361.
- Mildenhall, D. & Orpin, A. (2010) Terrestrial palynology from marine cores as an indicator of environmental change for the Waipaoa Sedimentary System and north-eastern New Zealand. *Marine Geology*, 270(1-4), 227–234.
- Moar N.T. (1993) *Pollen grains of New Zealand dicotyledonous plants*. Manaaki Whenua Press.
- Montade, V., Nebout, N.C., Kissel, C. & Mulsow, S. (2011) Pollen distribution in marine surface sediments from Chilean Patagonia. *Marine Geology*, 282(3-4), 161–168.
- Mountjoy, J.J., Barnes, P.M. & Pettinga, J.R. (2009) Morphostructure and evolution of submarine canyons across an active margin: Cook Strait sector of the Hikurangi Margin, New Zealand. *Marine Geology*, 260(1-4), 45–68.
- Mountjoy, J.J., Howarth, J.D., Orpin, A.R., Barnes, P.M., Bowden, D.A., Rowden, A.A. et al. (2018) Earthquakes drive large-scale submarine canyon development and sediment supply to deep-ocean basins. *Science Advances*, 4(3), eaar3748.
- Muller, J. (1959) Palynology of recent Orinoco delta and shelf sediments; reports of the Orinoco shelf expedition, 5. *Micropaleontology*, 5(1), 1–32.
- Nakagawa, T. (2007) PolyCounter ver. 1.0 & Ergodex DX-1: a cheap and very ergonomic electronic counter board system. *Quaternary International*, 167(Suppl), 298.
- National Institutes of Health (2023) ImageJ: Image processing and analysis in Java. Available at: <https://imagej.net/> [Accessed 30th August 2023].
- Orpin, A.R., Alexander, C., Carter, L., Kuehl, S. & Walsh, J. (2006) Temporal and spatial complexity in post-glacial sedimentation on the tectonically active, Poverty Bay continental margin of New Zealand. *Continental Shelf Research*, 26(17-18), 2205–2224.
- Paterson, G.A. & Heslop, D. (2015) New methods for unmixing sediment grain size data. *Geochemistry, Geophysics, Geosystems*, 16(12), 4494–4506.
- Piper, D.J. & Normark, W.R. (2009) Processes that initiate turbidity currents and their influence on turbidites: a marine geology perspective. *Journal of Sedimentary Research*, 79(6), 347–362.
- Pocknall, D.T. (1981a) Pollen morphology of the New Zealand species of *Dacrydium* Selander, *Podocarpus* L'Heritier, and *Dacrycarpus* Endlicher (Podocarpaceae). *New Zealand Journal of Botany*, 19(1), 67–95.
- Pocknall, D.T. (1981b) Pollen morphology of the New Zealand species of *Libocedrus* endlicher (Cupressaceae) and *Agathis* salisbury (Araucariaceae). *New Zealand Journal of Botany*, 19(3), 267–272.
- Pocknall, D.T. (1981c) Pollen morphology of *Phyllocladus* L.C. et A. Rich. *New Zealand Journal of Botany*, 19(3), 259–266.
- Pope, E.L., Cartigny, M.J., Clare, M.A., Talling, P.J., Lintern, D.G., Vellinga, A. et al. (2022) First source-to-sink monitoring shows dense head controls sediment flux and runout in turbidity currents. *Science Advances*, 8(20), eabj3220.
- Porro, F. (2018) Understanding palynomorph distribution in turbidite systems. PhD Thesis. University of Aberdeen.
- Pouderoux, H., Lamarche, G. & Proust, J. -N. (2012a) Building an 18 000-year-long paleo-earthquake record from detailed deep-sea turbidite characterisation in Poverty Bay, New Zealand. *Natural Hazards and Earth System Sciences*, 12(6), 2077–2101.
- Pouderoux, H., Proust, J. -N., Lamarche, G., Orpin, A. & Neil, H. (2012b) Postglacial (after 18 ka) deep-sea sedimentation along the Hikurangi Subduction Margin (New Zealand): characterisation, timing and origin of turbidites. *Marine Geology*, 295, 51–76.
- R Core Team. (2021) *R: a language and environment for statistical computing*. Vienna, Austria: R Foundation for Statistical Computing. <https://www.R-project.org/>
- Reilly, B., Stoner, J. & Wiest, J. (2017) Sed ct: Matlab™ tools for standardized and quantitative processing of sediment core computed tomography (CT) data collected using a medical CT scanner. *Geochemistry, Geophysics, Geosystems*, 18(8), 3231–3240.
- Roche, M. (1990) *History of New Zealand forestry*, New Zealand Forestry Corporation in association with GP Books.
- Roche M. (2008) *Exotic forestry. Te Ara—the encyclopedia of New Zealand*. Available at: <http://www.TeAra.govt.nz/en/exotic-forestry> [Accessed 20 November 2023].

- Star, P. (2008) Tree planting in Canterbury, New Zealand, 1850–1910. *Environment and History*, 14(4), 563–582.
- Stockmarr, J. (1971) Tables with spores used in absolute pollen analysis. *Pollen et spores*, 13, 615–621.
- Stow, D.A. & Bowen, A.J. (1980) A physical model for the transport and sorting of fine-grained sediment by turbidity currents. *Sedimentology*, 27(1), 31–46.
- Strachan, L.J., Bostock, H.C., Barnes, P.M., Neil, H.L. & Gosling, M. (2016) Non-cohesive silt turbidity current flow processes; Insights from proximal sandy-silt and silty-sand turbidites, Fiordland, New Zealand. *Sedimentary Geology*, 342, 118–132.
- Talling, P., Wynn, R., Masson, D., Frenz, M., Cronin, B., Schiebel, R. et al. (2007) Onset of submarine debris flow deposition far from original giant landslide. *Nature*, 450(7169), 541–544.
- Talling, P.J. (2013) Hybrid submarine flows comprising turbidity current and cohesive debris flow: deposits, theoretical and experimental analyses, and generalized models. *Geosphere*, 9(3), 460–488.
- Talling, P.J., Masson, D.G., Sumner, E.J. & Malgesini, G. (2012) Subaqueous sediment density flows: depositional processes and deposit types. *Sedimentology*, 59(7), 1937–2003.
- Tek, D.E., McArthur, A.D., Poyatos-Moré, M., Colombera, L., Allen, C., Patacci, M. et al. (2022) Controls on the architectural evolution of deep-water channel overbank sediment wave fields: insights from the Hikurangi Channel, offshore New Zealand. *New Zealand Journal of Geology and Geophysics*, 65(1), 141–178.
- Tomlinson, P. (1994) Functional morphology of saccate pollen in conifers with special reference to Podocarpaceae. *International Journal of Plant Sciences*, 155(6), 699–715.
- Tyson R.V. (Ed.) (1995) Distribution of the palynomorph group: sporomorph subgroup. In: *Sedimentary organic matter: organic facies and palynofacies*. Dordrecht: Springer, pp. 261–284.
- van den Bos, V., Newnham, R., Rees, A. & Woods, L. (2020) Density separation in pollen preparation: how low can you go? *Journal of Paleolimnology*, 63, 225–234.
- Vieira, M. & Jolley, D. (2020) Stratigraphic and spatial distribution of palynomorphs in deep-water turbidites: a meta-data study from the UK Central North Sea Paleogene. *Marine and Petroleum Geology*, 122, 104638.
- Walker, S., Price, R., Rutledge, D., Stephens, T. & Lee, W. (2006) Recent loss of indigenous cover in New Zealand. *New Zealand Journal of Ecology*, 30(1), 169–177.
- Wallace, L.M., Reyners, M., Cochran, U., Bannister, S., Barnes, P.M., Berryman, K. et al. (2009) Characterizing the seismogenic zone of a major plate boundary subduction thrust: Hikurangi Margin, New Zealand. *Geochemistry, Geophysics, Geosystems*, 10(10), 1–32.
- Wardle, P. (1991) *Vegetation of New Zealand*, CUP Archive.
- Webster, J.M., Beaman, R.J., Puga-Bernabéu, Á., Ludman, D., Renema, W., Wust, R.A. et al. (2012) Late Pleistocene history of turbidite sedimentation in a submarine canyon off the northern Great Barrier Reef, Australia. *Palaeogeography, Palaeoclimatology, Palaeoecology*, 331, 75–89.
- Wilmshurst, J.M. (1997) The impact of human settlement on vegetation and soil stability in Hawke's Bay, New Zealand. *New Zealand Journal of Botany*, 35(1), 97–111.
- Wilmshurst, J.M., Eden, D.N. & Froggatt, P.C. (1999) Late Holocene forest disturbance in Gisborne, New Zealand: a comparison of terrestrial and marine pollen records. *New Zealand Journal of Botany*, 37(3), 523–540.
- Woodhouse, A., Barnes, P.M., Shorrock, A., Strachan, L.J., Crundwell, M., Bostock, H.C. et al. (2022) Trench floor depositional response to glacio-eustatic changes over the last 45 ka, northern Hikurangi Subduction Margin, New Zealand. *New Zealand Journal of Geology and Geophysics*, 67(3), 312–335.